Fuel Processing Technology 201 (2020) 106319

Contents lists available at ScienceDirect

Fuel Processing Technology

journal homepage: www.elsevier.com/locate/fuproc

Conversion of furan over gallium and zinc promoted ZSM-5: The effect of metal and acid sites

Juliana S. Espindola[a,1], Christopher J. Gilbert[b,2], Oscar W. Perez-Lopez[a], Jorge O. Trierweiler[a], George W. Huber[b,*]

[a] Department of Chemical Engineering, Federal University of Rio Grande do Sul, Rua Luiz Englert s/n, Porto Alegre 90040-040, Brazil
[b] Department of Chemical and Biological Engineering, University of Wisconsin-Madison, 1415 Engineering Drive, Madison, WI 53706, United States of America

ARTICLE INFO

Keywords:
Furan conversion
Zinc
Gallium
ZSM-5
Acidity

ABSTRACT

The addition of gallium or zinc to ZSM-5 increases the aromatic selectivity and decreases the olefin selectivity for furan conversion. Both the benzene and naphthalenes selectivities increase with small amounts of gallium or zinc addition. At 5 wt% metal loading this effect is more pronounced with zinc promoted ZSM-5 having about 25% higher benzene selectivity than the gallium promoted ZSM-5. Additionally, the decarbonylation and methane formation reactions were both increased by adding zinc or gallium to the catalyst. As zinc or gallium loading is increased, the amount of Brønsted acid sites decrease, while the quantity of Lewis acid sites increase. This effect was more pronounced with zinc, as a result of its greater effectiveness to exchange with protons at the Brønsted acid sites. The aromatic yield appears to correlate with this increase in Lewis acidity. The addition of zinc to ZSM-5 also altered the reaction chemistry occurring during the hydrolysis of furan, lowering propylene and increasing methane yields as zinc loading increased.

1. Introduction

Catalytic fast pyrolysis (CFP) of biomass is receiving a tremendous amount of interest as a process to produce renewable aromatics and olefins [1–23]. CFP involves the thermal decomposition of biomass at high temperatures (typically between 500 and 600 °C), under an inert atmosphere in the presence of a zeolite catalyst (typically ZSM-5). It has been reported that [24–27] the cellulosic portion of biomass thermally decomposes into anhydrosugars, which are further converted by dehydration, decarbonylation, and decarboxylation reactions to produce oxygenated intermediates, including furanics. Furan has been used as a model compound to study the complicated catalytic reaction chemistry of CFP [24,28–33]. ZSM-5 has been shown to be the catalyst that produces the highest aromatic yield for CFP of biomass and model compounds due to its unique pore structure [24,25,27,28,30,34–39]. One potential method for increasing the aromatic yield is by the addition of bifunctional metal-oxide sites on ZSM-5. These additional sites can be added using either gallium [40–47] or zinc [47–51].

The effects of the addition of gallium to ZSM-5 have been previously studied for propane dehydrogenation and subsequent aromatization reactions [42,52–61]. Unsupported bulk Ga_2O_3 has been shown to catalyze dehydrocyclization (of n-hexene and 1,5-hexadiene to benzene), at a much greater rate than the dehydrogenation of propane [62]. However, the activity for propane dehydrogenation increases by two ordered of magnitude when gallium is added to ZSM-5 [54,55,57]. Gallosilicates (Ga_2O_3-SiO_2 mixtures analogous to aluminosilicate with the MFI structure) do not have any increased activity or selectivity for propane dehydrogenation *unless* additional gallium is deposited or the gallosilicate is steamed. Both of these treatments add extra-framework gallium to the zeolite (gallium species which are not located in the zeolite framework), which is apparently essential for increasing the dehydrogenation activity for this material [57].

Meriaudeau and Naccache [54] found that the sodium form of gallium-promoted ZSM-5 was inactive for propane conversion, either by dehydrogenation to propylene or by cracking to methane, while the dehydrogenation rate of propane to propylene was increased by 177.5 times when the protonated gallium-zeolite was used. These results suggest gallium does not create new Brønsted acid sites, but instead participates in a dual site mechanism involving gallium oxide and H^+ in Brønsted sites. Biscardi and Iglesia [61] suggested that the reduction

* Corresponding author.
E-mail address: gwhuber@wisc.edu (G.W. Huber).
[1] Present address: Escola de Química e Alimentos - Universidade Federal do Rio Grande. Rua Barão do Caí, 125 - Santo Antônio da Patrulha, Brazil - 95500-000.
[2] Present address: BASF Corporation - 25 Middlesex-Essex Turnpike, Iselin, NJ 08830.

https://doi.org/10.1016/j.fuproc.2019.106319
Received 16 August 2019; Received in revised form 2 December 2019; Accepted 12 December 2019

of extra-framework gallium oxide species (Ga_2O_3) in the presence of propane at high temperatures produced a mobile surface species (Ga_2O), which then enters the pores of the ZSM-5. According to these researchers, the active form of gallium for enhancement of dehydrogenation reactions is located in the ZSM-5 pores as a stable species attached to the oxygen atoms of the zeolite framework.

Propane aromatization with zinc promoted ZSM-5 has also been studied [49–51,55,61]. Increasing the loading of zinc on ZSM-5 (up to 1.3 wt%) was shown to increase the propane turnover rate, relative to aluminum sites, as well as the propene and benzene selectivity [50]. This is similar to behavior observed with gallium-promoted ZSM-5 catalysts [61]. According to Biscardi and Iglesia [61] both Ga and Zn promoted ZSM-5 catalysts effectively convert C6-C8 oligomers into the corresponding aromatics, while hindering further oligomerization or cracking reactions by increasing the rate of removal of intermediate compounds from the oligomerization-cracking cycle. However, adding zinc to ZSM-5 (0.5 wt%, ion exchange) decreases the cracking activity of the catalyst towards methane (this effect was not observed with a 5 wt% gallium/ZSM-5 catalyst) [55].

The addition of gallium [29,31,47,63,64,65,66] or zinc [47,66–71] to ZSM-5 for use in CFP has been previously studied. According to Cheng et al., [29] the addition of gallium increases the aromatic selectivity during furan conversion in a fixed bed reactor, while decreasing olefin and coke selectivity. Similar results were found by Uslamin et al., [31,63] for furan, 2-methylfuran and 2.5-dimethylfuran. Furthermore, gallium promoted ZSM-5 catalysts were found to increase the aromatic yield and selectivity for pinewood sawdust CFP in a bubbling fluidized bed [29] and for eucalyptus wood CFP in bubbling fluidized bed [64] or in a Py-GC–MS pyrolyzer [47]. Fanchiang and Lin [67] studied the furfural conversion over HZSM-5 impregnated with zinc, and observed the addition of this metal increased the aromatics, CO_2, and methane yield. Conversely, furan and propylene yields decreased. All of these effects were enhanced, with the exception of the shift in aromatic selectivity, which was independent of zinc loading, as the zinc loading was increased from 0.5 wt% to 1.5 wt% (catalysts prepared by incipient wetness impregnation) [67]. Studies with lignocellulosic biomass showed that zinc incorporation to ZSM-5 prevents the formation of undesired polyaromatic hydrocarbons and coke [68], increasing BTX yields and toluene selectivity [47,66,71].

The mechanism of furan conversion over ZSM-5 has been previously reported by our group and is shown in Scheme 1. Furan undergoes three reactions over ZSM-5: (1) Diels-Alder reaction with another furan to produce benzofuran and water, (2) decarbonylation to produce allene and CO, and (7) Diels-Alder condensation with an olefin to produce aromatics and water [28]. The incorporation of gallium to ZSM-5 does not create any new reaction pathway but increases the rate of aromatics production from furan by promoting the decarbonylation (2) and subsequent aromatization (3) reactions [29]. In the Scheme 1 the enhancement promoted by the presence of gallium is indicated by asterisk. The presence of water promotes furan hydrolysis and decomposition (4) to produce CO_2 and propylene [72].

The addition of gallium or zinc can affect the acidic properties of ZSM-5, and therefore it is important to consider the types of sites that could be formed. The types of acid sites present in unmodified ZSM-5, as well as the sites that may be formed upon addition of gallium or zinc that could contribute to the acidity of the catalyst are shown in Fig. 1a–c. Unmodified ZSM-5 contains both Brønsted (arising from the charge imbalance of aluminum substitution in the silica matrix) and Lewis acid sites (associated with hydroxyl groups attached to extra-framework alumina). The addition of gallium can create new Lewis acid sites from hydroxyls present on the surface of extra-framework gallium; analogous to the Lewis acid sites present in unmodified ZSM-5 due to extra-framework alumina. Adding zinc can reduce Brønsted acidity while simultaneously creating new Lewis acidity, since deposited zinc atoms can exchange with ZSM-5 sites. Exchanged zinc atoms have been found to be coordinated with four oxygen atoms (as determined by EXAFS) and may also be coordinated with a water molecule prior to heating (as determined by XANES) [50].

The addition of water has also been shown to affect unmodified [72] and gallium-promoted ZSM-5 [73]. Our previous report of the effect of water on conversion of furan over ZSM-5 [72], showed water promotes hydrolysis of furan to produce propylene and CO_2. These results were obtained under water vapor pressures close to what would be expected to occur with real biomass feed in a CFP process. Additionally, the co-feeding of small amounts of water with propane was found to increase conversion, selectivity towards aromatics, and dehydrogenation activity for gallium-promoted ZSM-5. However, the water partial pressures studied were all very low (< 30 Torr), and the optimal water partial pressure for enhancement of conversion was found to be 2.3 Torr [73].

The objective of this paper is to study how gallium and zinc promoted ZSM-5 catalysts influence the chemistry of furan conversion. The effect of water co-feeding on the activity of zinc-promoted catalysts was also investigated.

2. Experimental

2.1. Catalyst preparation

ZSM-5 obtained from Zeolyst (CBV 3024E, SiO_2/Al_2O_3 molar ratio: 30, NH_4-form) was used for preparation of the gallium or zinc promoted catalysts. The ZSM-5 was first calcined in a muffle furnace at 600 °C for 6 h to reach the acidic form of the zeolite (HZSM-5). Gallium nitrate (Sigma-Aldrich, $Ga(NO_3)_3{\cdot}8H_2O$ 99.9% purity) or zinc nitrate (Sigma-Aldrich, $Zn(NO_3)_2{\cdot}6H_2O$ 99% purity) were used as precursor salts, without further treatment. The appropriate amounts of each precursor were dissolved in deionized water (obtained in-house; amount of water based on observed point of incipient wetness of catalyst) to reach the desired loading of the metal species. Metal loadings prepared on the catalysts were as follows: 2 and 5 wt% Ga/ZSM-5 and 0.5, 1, 2 and 5 wt % Zn/ZSM-5. Table 1 shows the metal promoted catalysts, henceforth abbreviated as: 2Ga/ZSM-5, 5Ga/ZSM-5; 0.5Zn/ZSM-5, 1Zn/ZSM-5, 2Zn/ZSM-5 and 5Zn/ZSM-5, and composition obtained from mass balance, following the experimental procedure for catalyst preparation. The impregnated samples were dried overnight at 110 °C and then calcined in situ under air flow at 600 °C for 3 h. The catalysts were sieved to between 25 and 35 mesh (0.50 mm - 0.71 mm) before use. Unmodified ZSM-5 was calcined in situ at 600 °C for 3 h prior to use.

2.2. Catalyst characterization

The surface area and pore volume of the catalysts were measured by nitrogen adsorption at liquid nitrogen temperature using a Micromeritics surface area analyzer (ASAP model 2020). The samples were submitted to thermal treatment at 350 °C under vacuum for 8 h prior to the analysis. The surface area was obtained by assuming a pseudo-Langmuir isotherm, the micropore volume was obtained by t-plot, and the total pore volume was determined from a single point adsorption and desorption isotherms at partial pressure $P/P_o = 0.95$.

Temperature programmed desorption (TPD) experiments were performed in a Micromeritics analyzer (AutoChem model 2920 - Chemisorption Analyzer) using ammonia (NH_3) or isopropylamine (IPA). Prior to the analysis, calcined samples were subjected to thermal treatment at 600 °C under helium flow for 60 min, and then cooled. For NH_3-TPD, the sample was cooled to 150 °C, and then ammonia (15 vol %, balance helium; obtained from Airgas) was dosed at a flowrate of 50 mL/min for 30 min to ensure saturation. The sample cell was purged using 50 mL/min of pure helium (Airgas, UHP 5.0 grade) for 90 min prior starting the analysis. The thermal desorption of NH_3 was recorded by a thermal conductivity detector (TCD) during the 10 °C/min heating step from adsorption temperature to 600 °C, and then held at 600 °C for 60 min. For IPA-TPD, isopropylamine was dosed at 50 °C until

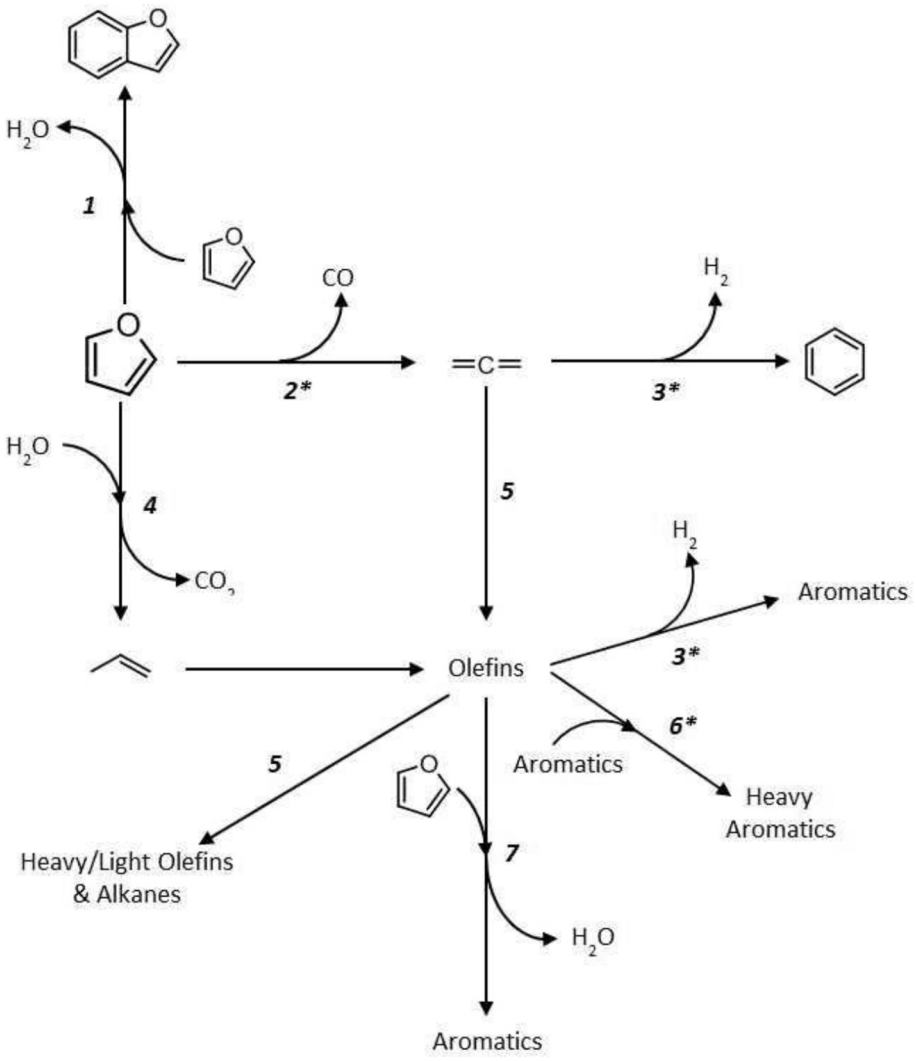

Scheme 1. Reaction network for furan conversion over ZSM-5 adapted from Cheng and Huber [28], Cheng et al. [29] and Gilbert et al. [72]. Reactions are indicated by numbers: (1) furan Diels-Alder self-condensation to produce benzofuran and water; (2) furan decarbonylation to produce CO and allene; (3) aromatization; (4) furan hydrolysis and decomposition to produce CO_2 and propylene; (5) oligomerization and cracking; (6) alkylation; and (7) Diels-Alder condensation between furan with olefins to produce aromatics and water. (*) indicates enhancement by the presence of gallium.

saturation. The sample cell was then purged using 50 mL/min of helium for 120 min prior starting the analysis. The desorbing gases were recorded by a TCD during the 10 °C/min heating step from adsorption temperature to 600 °C, and then held at 600 °C for 60 min. Brønsted acid sites in samples catalyze the decomposition of IPA into NH_3 and propylene at approximately 340 °C [74]. Framework substitution of gallium into the ZSM-5 matrix creates Brønsted acid sites that are also capable of catalyzing this decomposition at the same temperature [40].

2.3. Catalytic conversion of furan in a fixed bed reactor system

Reactions were performed in a continuous flow fixed bed reactor system capable of feeding a volatile reaction stream, as well dripping a second aqueous stream into the furnace over the catalyst bed. Both streams were fed using syringe pumps (Fisher, KDS100). Helium (Airgas, UHP 5.0 grade) was used as a carrier gas for reactions and was controlled by a mass flow controller (Brooks). Air (Airgas, industrial grade) was used for calcination and for combustion of the coke produced during reaction. It was dried by passing through a desiccant trap and the flow was adjusted by a needle valve and using a bubble flow meter. The catalyst was supported by a quartz frit inside a tubular quartz reactor. The reaction temperature was monitored by a thermocouple inserted inside the reactor located just above the catalyst bed. A condenser was placed after the reactor, although no liquid products were collected in this condenser. The non-volatile components were collected in gas bags. Fig. S1 shows the fixed bed reactor system used in the experiments.

The catalysts were calcined in situ with a heating rate of 4 °C/min to 600 °C for 3 h in air at a nominal flow rate of 60 mL/min. After calcination the system was flushed with 400 mL/min of helium for 10 min and the flow was then switched to bypass the reactor. Furan (Sigma-Aldrich, 99%) was pumped into the helium stream at a flow rate of 0.58 mL/h and this stream bypassed the reactor for 30 min. All reactions were performed at 600 °C for a reaction time of 4.5 or 6 min. In-house deionized water was used as the aqueous feed in experiments with water co-feeding.

Gaseous products were collected by gas bags, identified by GC–MS (Shimadzu-2010), and quantified by GC-FID/TCD (FID column: Restek, Rtx-VMS 40 m × 0.25 mmID × 1.4 μm; TCD column: Supelco Analytics, 80/100 Hayesep D 30 ft × 1/8 in × 2.1 mm).

Conversion was defined as the ratio between the moles of furan consumed in the reaction (furan present in the feed minus furan detected in the reactor effluent) and the moles of furan in the feed. Yield was defined as the amount of carbon present in the product species

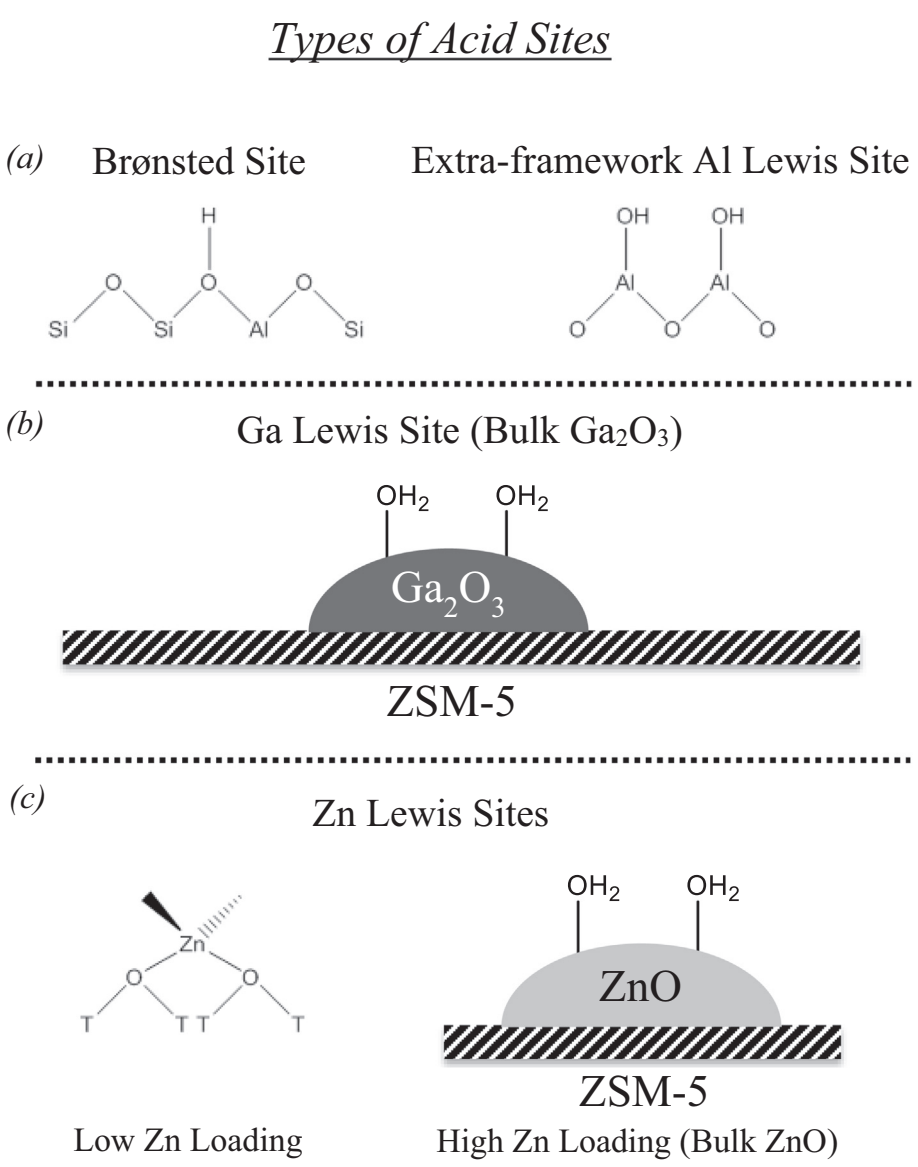

Fig. 1. a–c: Overview of the types of acid sites present in (a) unmodified ZSM-5, (b) proposed acid sites created by the addition of gallium, and (c) proposed acid sites created by the addition of zinc. Proposed low zinc loading sites adapted from Biscardi et al. [50]. The T's in (c) represent tetrahedrally coordinated aluminum or silicon atoms; dangling bonds from Zn atoms are to implied oxygen atoms.

divided by the amount of carbon present in the furan feed. Overall selectivity (of major product groups) was calculated based on the amount of carbon present in a product species divided by the total amount of carbon present in all products. Selectivity of individual species was calculated based on the amount of carbon present in a product species divided by the amount of carbon present in all product species of that type.

After reaction, the flow was switched to air for coke quantification.

Table 1
Physical properties of catalysts prepared for this study.

Catalyst	Metal	M (wt%)	M loading[a] (mmol/g)	M/Al Molar ratio	Surface area[b] (m^2/g)	Total pore Volume (cm^3/g)	Micropore volume[c] (cm^3/g)
ZSM-5	–	0.0	–	0.00	478	0.19	0.12
0.5Zn/ZSM-5	Zinc	0.5	0.076	0.07	487	0.20	0.12
1Zn/ZSM-5	Zinc	1.0	0.153	0.15	494	0.20	0.12
2Zn/ZSM-5	Zinc	2.0	0.306	0.30	480	0.25	0.11
5Zn/ZSM-5	Zinc	5.0	0.765	0.77	448	0.24	0.11
2Ga/ZSM-5	Gallium	2.0	0.287	0.29	451	0.18	0.13
5Ga/ZSM-5	Gallium	5.0	0.717	0.72	357	0.15	0.09

[a] Determined by mass balance following catalyst synthesis.
[b] Determined by assuming a pseudo-Langmuir isotherm.
[c] Determined by t-plot.

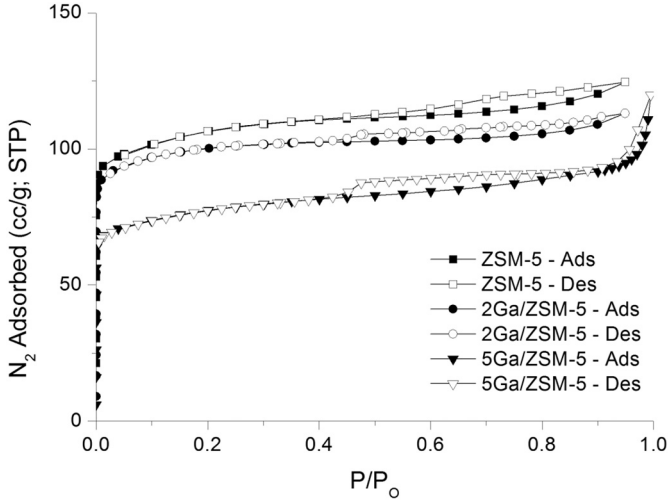

Fig. 2. Nitrogen physisorption isotherms of gallium promoted ZSM-5 catalyst samples performed at 77 K. Adsorption branches are represented by filled symbols; desorption branches are represented by open symbols.

The coke content was determined by combusting residual carbon and passing combustion products over a 13% CuO on Al_2O_3 (Sigma-Aldrich) converter to convert any CO to CO_2. The CO_2 was captured by the Ascarite (NaOH supported on silica, obtained from Sigma Aldrich) trap. The coke content was calculated from the mass difference of the Ascarite trap.

3. Results and discussion

3.1. Catalyst characterization

The nitrogen adsorption isotherms for gallium promoted ZSM-5 catalysts are shown in Fig. 2; the adsorption isotherms for zinc promoted ZSM-5 catalysts are shown in Fig. 3a–d. A summary of the textural properties of the catalysts is given in Table 1. The XRD patterns of the catalysts are presented in Fig. S2.

As can be seen in Fig. 2 and Table 1, the addition of gallium to ZSM-5 causes a decrease in the nitrogen uptake. This decrease is most noticeable at the 5 wt% loading for surface area and micropore volume. The micropore volume decreases from 0.12 cm^3/g for the pure ZSM-5 catalyst to 0.09 cm^3/g for the 5 wt% Ga/ZSM-5 catalyst, while the surface area decreased from 478 to 357 m^2/g. The decrease in the nitrogen uptake from the addition of 2 wt% gallium is much smaller, and there is no apparent change in micropore volume. This suggests that increased loading of gallium on ZSM-5 (such as 5 wt%) may lead to pore blockage. In contrast the nitrogen uptakes for the zinc promoted catalysts were all similar to the unmodified ZSM-5 and approximately the same, as shown in Fig. 3a–d. A small decrease in nitrogen uptake is observed for 5 wt% zinc loading (Fig. 3d), which suggests a small amount of pore blockage. This suggests that gallium is more likely to block pores of the ZSM-5 than zinc. The XRD patterns of samples show the addition of gallium or zinc did not affect the ZSM-5 framework (Fig. S2). No extra peak was observed for the impregnated catalysts, which indicates the metals are highly dispersed on the ZSM-5 surface.

An overview of the acidic properties of the catalyst samples is given in Table S1 and shown in Fig. 4. The addition of zinc to ZSM-5 reduces

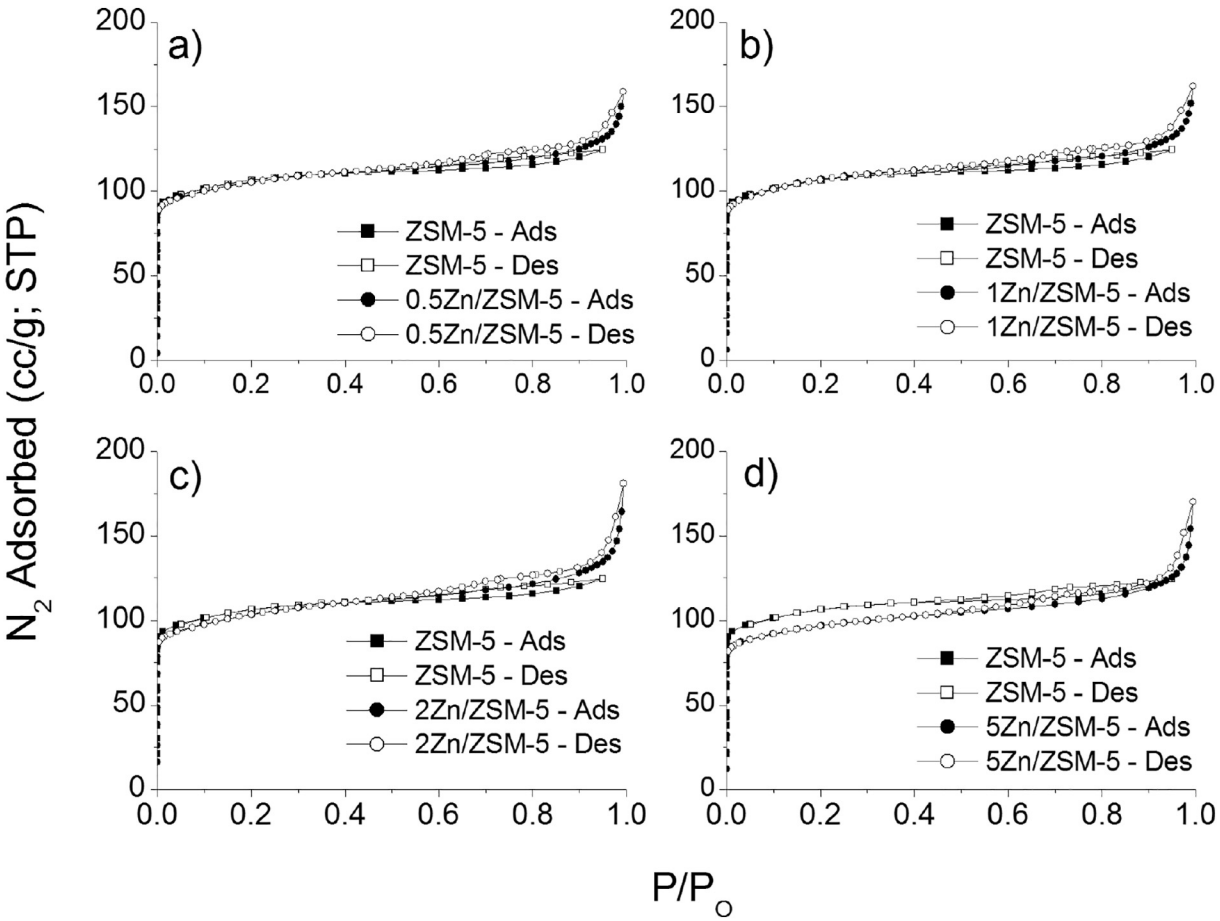

Fig. 3. a–d: Nitrogen physisorption isotherms of zinc promoted ZSM-5 catalyst samples performed at 77 K. Adsorption branches are represented by filled symbols; desorption branches are represented by open symbols for (a) 0.5Zn/ZSM-5, (b) 1Zn/ZSM-5, (c) 2Zn/ZSM-5 and (d) 5Zn/ZSM-5.

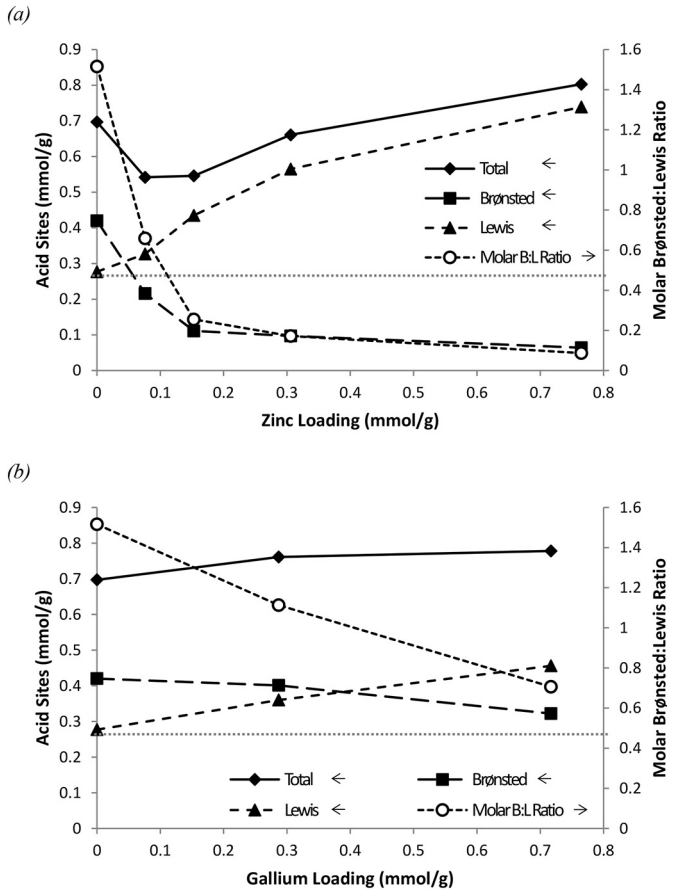

Fig. 4. a–b: Distribution of acid sites of ZSM-5 impregnated with (a) zinc and (b) gallium. Total acid sites were determined by ammonia TPD; Brønsted sites were determined by the IPA-TPD method developed by Kofke et al. [74]; Lewis sites were determined by difference between total acid sites and Brønsted acid sites. The dotted grey line represents the amount of Lewis sites present in unmodified ZSM-5.

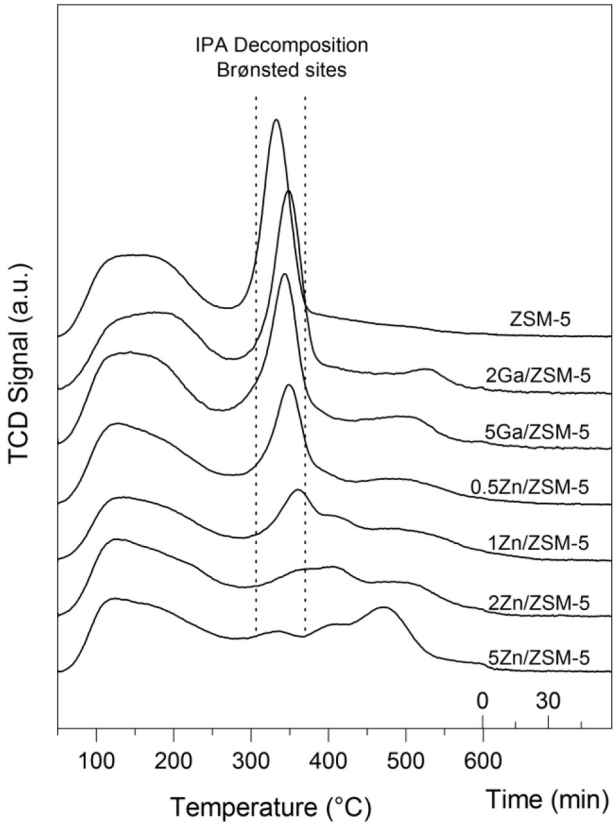

Fig. 5. IPA-TPD profiles for the catalyst samples. Samples were heated at 10 °C/min to 600 °C, and then held for 60 min at that temperature. The peak at approximately 340 °C (shown between the dotted lines) corresponds to Brønsted acid site catalyzed decomposition of IPA into propylene and ammonia [74].

the concentration of Brønsted acid sites while creating new Zn Lewis sites. These results are in agreement with those from Berndt et al. [49] and Biscardi et al. [50], that proposed the formation of zinc-exchanged Lewis sites (Fig. 1c – Low Zn Loading) during calcination by solid state exchange of protons in samples prepared by impregnation [49]. The total acidity of zinc promoted catalysts passes through a minimum between 0.5 wt% and 1 wt% zinc, as depicted in Fig. 4a. Gallium, on the other hand, does not show such a dramatic decrease in the quantity of Brønsted sites at comparable metal loadings (0.401 mmol/g with 2 wt% gallium compared to 0.097 mmol/g with 2 wt% zinc). Additionally, there are fewer Lewis acid sites created compared to zinc (0.360 mmol/g with 2 wt% gallium, as opposed to 0.565 mmol/g with 2 wt% zinc) at the same loadings.

The IPA-TPD is shown in Fig. 5. The IPA decomposition into propylene and NH_3, and their subsequent desorption, occurs at approximately 340 °C [74]. In all of the metal promoted catalyst samples, some additional peaks can be seen at higher temperatures that are not present during the analysis of unmodified ZSM-5. Gallium promoted catalysts typically have a single high temperature peak at approximately 500 °C. The addition of zinc at loadings above 1 wt% creates multiple high temperature peaks. There are three possible origins for these peaks: (1) desorption of unreacted chemisorbed IPA; (2) higher temperature acid catalyzed decomposition of IPA into propylene and NH_3; or (3) readsorption of NH_3 produced from the decomposition of IPA at approximately 340 °C, and then subsequent desorption. Each of these different possibilities has different implications regarding the acidic nature of the catalysts. In the first case, it is possible that the addition of metals creates acid sites that are capable of retaining IPA to higher temperatures (the broad low temperature peak between 100 and 200 °C is desorbing chemisorbed IPA [46]). In this case, it would seem likely that these sites are Lewis in character, since these sites would be too weak to catalyze decomposition of IPA. If the second possibility were true, then it is possible that the new sites are strong Lewis acid sites capable of catalyzing the decomposition of IPA, albeit at a higher temperature than the Brønsted sites already present. Lastly, in the third case, it is not possible to comment on the nature of acid sites, other than to suggest they are strong acid sites. A previous study [46] using a similar characterization technique with a mass spectrometer, observed a shoulder in the NH_3 desorption signal with 3 wt% Ga-ZSM-5 at approximately 500 °C [46]. This suggests that the high temperature peaks observed during our IPA-TPD may be related to new Lewis sites present on the surface of the ZSM-5 created by bulk Ga_2O_3 or ZnO (Fig. 1b and c).

The NH_3-TPD TCD responses are shown in Fig. 6. Two distinct peaks are observed for sample ZSM-5. The lower temperature peak, centered at approximately 225 °C, corresponds to ammonia desorbing from weaker acid sites. The higher temperature peak, centered at approximately 385 °C, corresponds to ammonia desorbing from stronger acid sites. Zinc promoted catalysts show widening of low temperature peak suggesting the formation of zinc species of weak acidity with increasing Zn loadings. The high temperature peak shows a decrease in intensity for all zinc promoted samples and a shoulder towards higher temperatures for 2 and 5 wt% zinc loading. These results indicate a decrease in amount of strong acid sites, possibly related to new Lewis sites created by bulk ZnO. Gallium promoted catalysts showed smaller changes in the ammonia TPD profile. The high temperature peak shows a decrease in intensity while low temperature peak became wider for both samples. The observed results are in agreement with the observed

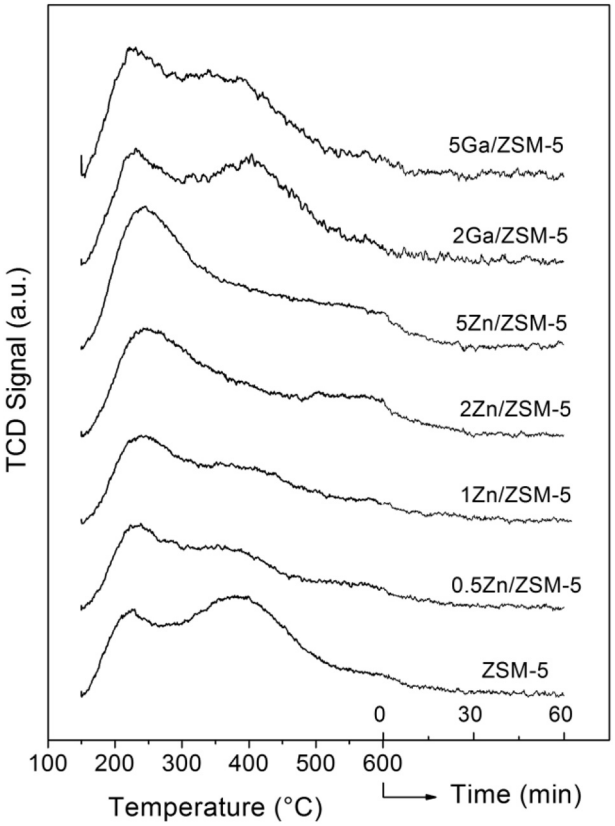

Fig. 6. NH_3-TPD profiles for the catalyst samples. The samples were heated at 10 °C/min to 600 °C, and then held for 60 min at that temperature.

results of IPA-TPD (Fig. 5).

3.2. Effect of addition of Ga/Zn on the CFP of furan

A summary of the effects of the addition of zinc or gallium on the CFP of furan in a fixed bed reactor is shown in Table 2. The furan conversion increased from 46.1% for ZSM-5 to 52.5% and 69.5% for 2Ga/ZSM-5 and 5Zn/ZSM-5, respectively. The addition of gallium or zinc also improved results for aromatics production particularly increasing the benzene yield.

As shown in Table 2, the presence of both metals, gallium and zinc, enhance furan decarbonylation and aromatization reactions, increasing the rate of aromatics production from furan. According to Scheme 1, furan undergo decarbonylation to produce allene. The allene can either undergo dimerization and aromatization reactions (Scheme 1 - pathway 3) or oligomerization, cracking and aromatization reactions (Scheme 1 - pathways 5 and 3) to produce aromatics. The promoting effect of gallium and zinc over aromatics production is attributed to the promotion of effective hydrogen transfer, increasing the rate of dehydrogenation reactions and promoting benzene production from olefins while hindering further oligomerization or cracking reactions [29,51,61]. Furthermore, both metals have been found to inhibit cracking side reactions that lead to undesirable products [51,61], increasing the selectivity of aromatization reactions. They also promote olefins alkylation with aromatics to form heavy aromatics.

The addition of gallium to unmodified ZSM-5 catalyst increases selectivity towards aromatics, CO, and methane, while decreasing selectivity towards olefins. Increasing the gallium loading from 2 wt% to 5 wt% does not appear to alter the product distribution any further. The increase in the aromatic selectivity is entirely due to an increase in benzene and naphthalenes production. There is also an increase in allene production, as well as decreases in ethylene and propylene production, resulting in a noticeable shift in olefin selectivity towards allene. This increase is likely coupled with the increase in CO production (removal from furan), as allene can be produced by decarbonylation of furan. The addition of gallium to ZSM-5 also appears to increase oxygenate selectivity towards benzofuran. The results obtained from the CFP of furan over gallium promoted ZSM-5 catalysts are in agreement with previously reported findings [29].

The effects of the addition of zinc to ZSM-5 on the CFP of furan are similar in scope, but differ in magnitude, to the changes observed with gallium. Zinc increases the selectivity towards aromatics, CO, and methane. Selectivity towards olefins and coke decreases with zinc addition. Furan conversion also noticeably increases. However, the increase in aromatic selectivity at 5 wt% metal loading is much greater with zinc (about a 17% increase) than with gallium (only about an 8% increase). Similar trends are observed with CO (5% with zinc; 2% with gallium) and methane (0.8% with zinc; 0.1% with gallium). The decrease in olefin selectivity is also more pronounced with zinc (11% with zinc; 6% with gallium). Like gallium, zinc increases benzene selectivity among aromatics, but the effect is much more substantial than the gallium effect. Likewise, the changes in aromatic selectivity are due to increases in benzene production, rather than decreases in yields of any other species. Furthermore, a significant increase in allene selectivity is observed; with zinc promoted catalysts, allene is the predominant olefin species (up to 47%) at zinc loadings above 2 wt%. An increase in benzofuran selectivity is observed among oxygenates; however, in this case, the magnitude of the change is comparable to results obtained with gallium. There was a large decrease in coke selectivity with zinc promoted catalysts, while no significant change was observed with gallium promoted catalysts. However, this result may be related to the difference in the magnitude of the effects between the two metals, which produces catalysts with great difference in the acidic properties at similar molar loadings, as can be seen in Table S1 for Brønsted to Lewis ratio: 0.172 with zinc (0.306 mmol Zn/g) and 1.113 with gallium (0.287 mmol Ga/g). Although zinc and gallium exhibit similar behavior on furan CFP, zinc has a much greater effect at the same loading. It appears to be more effective at decarbonylation and aromatization (cyclization) than gallium at the same loadings.

The change in activity of the different catalysts may be related to the difference in their acidic properties. This raises the question: are the differences in the product distributions observed caused by inherit differences in the metal species active sites, or is it due to the altering of the acidic properties of the catalyst? Consider 0.5Zn/ZSM-5 and 5Ga/ZSM-5; these catalysts have similar acidic properties (and a similar ratio of Brønsted to Lewis acid sites). The conversion and selectivity of aromatic, olefin, and oxygenate species are quite similar between the two different catalysts. However, the overall selectivity to aromatics and olefins each differ by only 5% between the two catalyst samples. This suggests that the observed results are due to changes in the catalyst acidity. It is also worth noting that the 0.5Zn/ZSM-5 only appears to have single high temperature IPA-TPD peak (shown in Fig. 6), similar to gallium promoted catalysts.

The mechanism of furan conversion over ZSM-5 catalysts, described in our previous work [28,30], shows the first step in furan conversion over ZSM-5 is either the Brønsted activated decarbonylation reaction in which C-O-C bond is broken to produce allene and CO or the Diels-Alder reaction with another furan to produce benzofuran and water. After that, the Brønsted acid sites activate the isomerization and cracking reactions which lead to the production of olefins. Once the reactional system contains olefins available, the olefins undergo further reactions producing single-ring and poly-ring aromatics and coke. The Diels-Alder condensation consumes olefins and furan to produce aromatic compounds and water. The aromatization is a Lewis promoted reaction that involves olefin alkylation to chain growth and cyclization. As the reactions show, both acid sites are important in the CFP of furan over ZSM-5 and the addition of metallic acid sites to the catalyst can have significant effect over the reaction yield and selectivity since it

Table 2
The effect of metal loading on the overall product yields and individual product selectivities of the CFP of furan over ZSM-5 and M/ZSM-5. Experiments carried out at 600 °C with a furan partial pressure of about 6 Torr, total system pressure 760 Torr, reaction time 4.5 min, WHSV = 9.3 h^{-1}. One standard deviation is given next to the main entry in the table. All value for yields/selectivities are in % carbon.

Catalyst	ZSM-5	0.5Zn/ZSM-5	1Zn/ZSM-5	2Zn/ZSM-5	5Zn/ZSM-5	2Ga/ZSM-5	5Ga/ZSM-5
Conversion (%)	46.1 ± 2.2	49.8 ± 2.2	66.9 ± 2.3	53.0 ± 3.3	69.5 ± 1.0	52.5 ± 1.1	46.5 ± 1.8
Coke on catalyst (%)	5.7 ± 0.4	5.6 ± 0.1	5.5 ± 0.9	4.5 ± 0.7	4.9 ± 0.3	5.7 ± 0.5	5.6 ± 0.1
Overall yield (%C)							
Aromatics	7.9 ± 0.3	10.8 ± 0.3	16.8 ± 1.8	13.2 ± 0.9	19.6 ± 0.7	11.0 ± 0.6	12.1 ± 0.1
Olefins	9.9 ± 0.4	11.9 ± 0.1	10.5 ± 0.5	9.4 ± 0.9	7.6 ± 0.3	7.9 ± 0.4	8.3 ± 0.2
Oxygenates[a]	0.7 ± 0.1	1.1 ± 0.1	0.6 ± 0.0	0.7 ± 0.2	0.6 ± 0.1	0.5 ± 0.1	0.8 ± 0.0
CO	6.8 ± 0.2	8.6 ± 0.1	13.9 ± 1.0	10.4 ± 0.4	13.0 ± 0.5	9.0 ± 0.2	8.3 ± 0.1
CO_2	1.0 ± 0.0	1.3 ± 0.1	0.7 ± 0.1	0.9 ± 0.1	1.1 ± 0.1	0.9 ± 0.2	1.0 ± 0.2
Methane	0.0 ± 0.0	0.3 ± 0.1	0.6 ± 0.1	0.6 ± 0.1	0.8 ± 0.1	0.1 ± 0.0	0.2 ± 0.0
Coke	11.6 ± 0.8	11.4 ± 0.1	11.1 ± 1.8	9.2 ± 1.4	10.0 ± 0.6	11.5 ± 1.0	11.4 ± 0.2
Aromatics + olefins yield (%)	17.7 ± 0.7	22.7 ± 0.4	27.3 ± 1.3	22.6 ± 0.8	27.2 ± 1.0	18.8 ± 0.2	20.4 ± 0.3
Overall selectivity (%C)							
Aromatics	20.8 ± 0.3	23.9 ± 0.4	31.0 ± 0.9	29.8 ± 2.0	37.1 ± 0.8	26.7 ± 2.3	28.7 ± 0.1
Olefins	26.2 ± 0.4	26.1 ± 0.1	19.5 ± 2.5	21.2 ± 2.4	14.5 ± 0.3	19.2 ± 0.4	19.7 ± 0.4
Oxygenates[a]	1.8 ± 0.2	2.5 ± 0.1	1.1 ± 0.1	1.6 ± 0.4	1.1 ± 0.1	1.1 ± 0.1	1.9 ± 0.0
CO	17.9 ± 0.4	18.9 ± 0.0	25.6 ± 0.2	23.3 ± 0.6	24.7 ± 0.6	22.0 ± 1.2	19.8 ± 0.3
CO_2	2.6 ± 0.2	2.8 ± 0.2	1.3 ± 0.1	2.1 ± 0.3	2.2 ± 0.3	2.2 ± 0.5	2.5 ± 0.4
Methane	0.1 ± 0.1	0.7 ± 0.2	1.1 ± 0.1	1.3 ± 0.2	1.6 ± 0.2	0.3 ± 0.1	0.4 ± 0.0
Coke	30.6 ± 0.8	25.2 ± 0.6	20.4 ± 1.7	20.8 ± 2.7	18.9 ± 1.1	28.0 ± 1.6	27.1 ± 0.6
Aromatics + olefins selectivity (%)	47.0 ± 0.3	50.0 ± 0.4	50.4 ± 1.6	51.0 ± 2.6	51.6 ± 0.9	45.8 ± 1.9	48.5 ± 0.5
Aromatic selectivity (%C)							
Benzene	40.4 ± 0.9	46.8 ± 0.7	67.0 ± 2.0	64.1 ± 3.4	73.9 ± 0.9	54.7 ± 5.0	48.5 ± 2.2
Toluene	34.8 ± 0.8	21.1 ± 0.1	14.6 ± 0.2	14.7 ± 0.8	12.3 ± 0.1	26.0 ± 2.6	23.3 ± 0.7
Ethylbenzene	0.8 ± 0.0	0.8 ± 0.0	0.6 ± 0.1	0.5 ± 0.1	0.3 ± 0.0	0.4 ± 0.1	0.4 ± 0.0
Xylenes[b]	3.3 ± 0.1	4.3 ± 0.3	5.0 ± 0.1	4.2 ± 0.5	3.0 ± 0.3	2.0 ± 0.1	2.2 ± 0.0
Styrene	7.5 ± 0.2	5.0 ± 0.0	2.8 ± 0.1	3.8 ± 0.4	2.6 ± 0.1	7.6 ± 1.6	7.6 ± 0.6
Indene	8.2 ± 0.4	8.3 ± 0.3	4.0 ± 0.2	5.1 ± 0.6	4.5 ± 0.3	5.8 ± 0.7	8.4 ± 0.2
Naphthalenes[c]	5.0 ± 1.4	13.6 ± 0.7	6.0 ± 1.4	7.6 ± 1.7	3.5 ± 0.5	3.6 ± 0.1	9.7 ± 0.8
Olefin selectivity (%C)							
Ethylene	36.0 ± 0.6	29.9 ± 0.0	33.5 ± 0.7	21.4 ± 1.0	25.5 ± 1.4	36.9 ± 0.6	31.3 ± 0.9
Propylene	36.3 ± 0.2	27.6 ± 0.5	20.9 ± 0.3	12.6 ± 0.5	18.4 ± 0.6	31.7 ± 5.0	27.6 ± 2.1
Allene	7.4 ± 0.2	24.8 ± 0.0	30.2 ± 0.2	46.8 ± 0.4	39.8 ± 0.9	15.5 ± 5.4	22.3 ± 1.3
Butenes[d]	5.4 ± 0.1	9.1 ± 0.0	8.6 ± 0.1	11.4 ± 0.3	8.9 ± 0.1	5.7 ± 0.6	8.5 ± 0.0
Cyclopentadiene[e]	13.3 ± 0.2	7.5 ± 0.1	5.4 ± 0.2	5.8 ± 0.3	5.6 ± 0.4	9.5 ± 0.2	9.6 ± 0.0
Hexenes	1.5 ± 0.2	1.2 ± 0.0	1.4 ± 0.0	2.0 ± 0.1	1.8 ± 0.1	0.7 ± 0.2	0.7 ± 0.0
Oxygenates selectivity (%C)							
Benzofuran	55.0 ± 2.4	76.8 ± 1.2	62.9 ± 0.6	79.6 ± 2.4	77.0 ± 2.2	66.3 ± 2.1	76.8 ± 1.5
Acetone	3.7 ± 0.1	6.0 ± 0.9	7.8 ± 1.1	5.4 ± 1.6	3.4 ± 1.6	N/A	6.5 ± 0.3
Acetaldehyde	3.8 ± 0.4	2.4 ± 0.3	1.9 ± 0.9	1.5 ± 0.3	1.7 ± 1.7	2.2 ± 0.5	1.3 ± 0.1
2-methylfuran	32.0 ± 2.4	9.6 ± 0.1	13.2 ± 1.5	5.0 ± 0.3	4.8 ± 0.4	25.8 ± 2.8	10.8 ± 0.1
Phenol	8.3 ± 2.8	5.3 ± 0.1	14.3 ± 0.1	8.4 ± 0.6	13.0 ± 1.1	5.7 ± 1.3	4.6 ± 1.2

[a] Defined as any oxygen containing molecule other than CO or CO_2.
[b] Includes all three xylene isomers.
[c] Naphthalenes includes naphthalene, 1-methylnaphthalene and 2-methylnaphthalene.
[d] Includes 1-butene, 2-butene, isobutene, and butadiene.
[e] Only C_5 olefin detected in significant quantities.

affect the type and number of acid sites, the density of Brønsted and Lewis sites and the strength of acid sites, as shown in Figs. 4 and 5. From that, it is expected that some of the products correlate with the Brønsted acidity, the Lewis acidity or with the Brønsted to Lewis ratio.

The effect of Lewis acid sites on products yield is presented in Fig. S3a–d and Fig. S4a–c. The aromatics increase with increasing Lewis acidity (Fig. S3a) by 12%. The olefin (Fig. S3b) and coke (Fig. S3d) yields both seem to be independent of Lewis acidity, while the CO presented and increase of 6% (Fig. 3c). No strong correlation between CO_2, oxygenate, or methane yields (Fig. S4a–c) and Lewis acidity was observed. As expected from the reactions involved in furan conversion over ZSM-5, a positive correlation between Lewis acid sites and aromatics yield can be observed. The aromatics selectivity (Table 2) increase with the increase in Lewis acid sites (Table S1) and follows: ZSM-5 < 0.5Zn < 1Zn ≤ 2 Zn < 5 Zn; ZSM-5 < 2 Ga < 5Ga. The effect of Brønsted acid sites on product yields are shown in Fig. S5a-d and Fig. S6a-c. As shown in Fig. S5a, aromatic yields decrease by 12% with increasing Brønsted acidity, whereas CO yield (Fig. S5c) shows a 6% decrease with increasing Brønsted acidity. Olefin (Fig. S5b) and coke (Fig. S5d) yields appear to be independent of Brønsted acidity. It appears that methane yield (Fig. S6c) has a strong negative correlation with respect to increasing Brønsted acidity. No correlation between CO_2 (Fig. S6a) or oxygenate (Fig. S6b) yields and Brønsted acidity was observed. Although olefins are produced by a Brønsted activated reaction, they participate in a series of reactions, being consumed in Lewis and Brønsted activated reactions. Hence, our results do not provide a correlation between olefins yield and Brønsted acid sites.

3.3. Effect of water on conversion of furan over Zn/ZSM-5

Table 3 shows the effects of steam on the conversion of furan over ZSM-5 with varying zinc loadings. The effect of water on increasing the rate of furan hydrolysis decreases with increasing addition of zinc to ZSM-5. Water also reduces the selectivity to aromatics and coke irrespective of zinc loading. The oxygenate selectivity is increased in the presence of water as zinc loading is increased, with acetone showing a dramatic increase with water addition. The combined aromatics + olefins selectivity in the presence of water appears to pass through a maximum at a loading of 0.5 wt% Zn, before decreasing sharply as the zinc loading is increased.

Table 3
The effect of co-feeding water with furan over catalysts with varying zinc contents on overall product yields and individual product selectivities. Experiments carried out for 6 min at 600 °C with a furan partial pressure of about 6 Torr, total system pressure of 760 Torr, WHSV = 9.3 h^{-1}. One standard deviation is given next to the main entry in the table, when available. All values for yields/selectivities are in % carbon.

Catalyst	ZSM-5		0.5Zn/ZSM-5		1Zn/ZSM-5		2Zn/ZSM-5		5Zn/ZSM-5	
H_2O partial pressure (Torr)	0	130	0	131	0	132	0	130	0	132
Conversion (%)	43.8	73.1 ± 4.7	41.4	67.4 ± 2.7	58.6	68.1	48.8	56.6	66.3	61.3
Coke on catalyst (%)	7.8	8.1 ± 1.6	5.7	2.9 ± 0.7	6.9	4.3	5.9	3.6	5.4	2.8
Overall yields (%C)										
Aromatics	7.8	6.8 ± 0.7	9.5	6.6 ± 2.0	13.3	8.4	10.1	7.6	17.0	8.8
Olefins	8.1	30.6 ± 3.1	11.1	32.2 ± 4.5	10.2	22.6	9.9	16.8	7.9	10.4
Oxygenates[a]	1.0	1.3 ± 0.1	1.1	1.6 ± 0.3	0.6	1.6	0.6	1.9	0.5	2.0
CO	5.8	6.2 ± 1.4	7.8	6.3 ± 1.1	12.0	9.7	9.3	8.3	12.3	10.1
CO_2	0.7	8.9 ± 0.4	1.0	9.5 ± 1.0	0.6	7.1	0.6	7.8	0.9	9.8
Methane	0.0	0.2 ± 0.0	0.1	0.6 ± 0.2	0.5	2.6	0.4	4.6	0.7	9.3
Coke	11.9	12.4 ± 2.4	8.8	4.4 ± 1.0	10.5	6.6	9.0	5.2	8.3	4.2
Aromatics + olefins yield (%C)	15.9	37.5 ± 3.8	20.6	38.9 ± 6.6	23.5	31.0	20.0	24.4	24.8	19.2
Overall selectivity (%C)										
Aromatics	22.0	10.3 ± 0.2	24.0	10.7 ± 1.5	27.4	13.7	25.2	14.5	35.8	16.1
Olefins	23.0	46.2 ± 0.7	28.3	52.8 ± 1.4	20.9	37.6	24.9	32.2	16.5	19.1
Oxygenates	2.9	2.0 ± 0.5	2.8	2.5 ± 0.0	1.1	2.9	1.4	3.7	1.1	3.7
CO	16.5	9.2 ± 1.0	19.8	10.4 ± 0.1	24.7	15.7	23.4	15.9	26.0	18.4
CO_2	2.1	13.4 ± 1.0	2.6	15.6 ± 1.0	1.2	12.8	1.6	15.0	1.9	17.9
Methane	0.0	0.3 ± 0.0	0.2	0.9 ± 0.2	1.1	4.0	1.0	8.9	1.4	17.0
Coke	33.6	18.6 ± 1.4	22.3	7.1 ± 0.5	21.3	10.9	22.5	9.9	17.4	7.8
Aromatics + olefins selectivity (%C)	44.9	56.5 ± 0.9	52.4	63.5 ± 0.2	48.3	51.4	50.1	46.7	52.3	35.2
Aromatic selectivity (%C)										
Benzene	33.6	33.4 ± 0.3	44.9	48.2 ± 2.3	66.9	56.1	65.3	60.0	73.6	68.1
Toluene	27.7	42.7 ± 3.2	20.6	32.2 ± 1.0	14.6	21.6	15.4	18.1	12.0	15.4
Ethylbenzene	0.8	1.1 ± 0.1	0.8	1.2 ± 0.1	0.6	0.8	0.6	0.6	0.3	0.6
Xylenes[b]	3.4	6.6 ± 0.7	3.7	5.6 ± 0.8	4.7	4.8	4.3	4.9	3.3	4.1
Styrene	6.9	5.0 ± 1.1	5.1	3.0 ± 0.1	2.7	3.1	3.8	3.4	2.5	2.3
Indene	15.0	4.4 ± 1.0	8.4	3.2 ± 0.0	4.0	4.0	4.3	4.0	4.3	3.0
Naphthalenes[c]	12.7	6.7 ± 4.4	16.6	6.7 ± 0.3	6.6	9.5	6.4	9.1	4.0	6.5
Olefin selectivity (%C)										
Ethylene	37.5	13.2 ± 3.4	28.2	7.4 ± 1.0	29.6	14.9	19.5	14.3	24.1	16.8
Propylene	35.3	73.4 ± 3.0	24.9	73.4 ± 0.6	20.0	58.8	11.6	46.9	15.9	39.0
Allene	5.7	1.1 ± 0.4	28.7	1.9 ± 0.6	34.6	5.8	50.0	12.3	43.6	20.7
Butenes[d]	4.7	8.1 ± 0.3	9.2	14.4 ± 0.3	8.6	17.1	11.1	23.2	9.0	19.6
Cyclopentadiene[e]	14.6	3.1 ± 0.1	7.8	2.4 ± 0.2	5.8	3.0	5.6	2.9	5.4	3.1
Hexenes	2.2	1.0 ± 0.2	1.2	0.5 ± 0.1	1.5	0.4	2.2	0.5	1.9	0.9
Oxygenates selectivity (%C)										
Benzofuran	47.5	9.6 ± 6.5	76.5	11.7 ± 0.2	58.0	12.8	76.7	12.8	75.8	9.0
Acetone	N/A	28.1 ± 1.8	4.7	58.2 ± 1.5	7.9	64.8	6.3	71.3	2.5	79.1
Acetaldehyde	7.7	46.9 ± 1.8	2.2	21.2 ± 1.0	2.0	14.1	1.7	11.1	1.0	6.8
2-methylfuran	33.1	6.9 ± 1.0	10.8	3.3 ± 0.5	17.1	4.3	6.9	1.6	5.7	1.5
Phenol	9.1	8.5 ± 2.0	5.7	5.6 ± 1.2	15.1	4.0	8.4	3.2	15.1	3.6

[a] Defined as any oxygen containing molecule other than CO or CO_2.
[b] Includes all three xylene isomers.
[c] Naphthalenes includes naphthalene, 1-methylnaphthalene and 2-methylnaphthalene.
[d] Includes 1-butene, 2-butene, isobutene, and butadiene.
[e] Only C_5 olefin detected in significant quantities.

The effects of zinc loading on the yields of four important species (both with and without water co-feed) are shown in Fig. S7a–d. The CO_2 yield is independent of zinc loading in the presence of water. However, it is quite apparent that zinc has a dramatic effect on propylene with the propylene yield reduced by nearly 20%C as the zinc loading increases to 5 wt% (Fig. S7a). Even in the absence of water, there appears to be a decrease in propylene yield. Counterintuitively, there is no corresponding increase in benzene yield that would be present if the zinc was promoting aromatization of propylene to benzene (through dehydrocylcization; see Fig. S7c). It is the combination of these two changes that is the primary effect on the combined aromatic + olefin selectivity. Methane yield increases as zinc loading increases (Fig. S7d). It would appear that the behavior of zinc impregnated on ZSM-5 is altered by the presence of water. This may be related to behavior observed by Biscardi et al. using X-ray absorption. These authors noted that the Zn species in Zn/ZSM-5 catalysts undergoes a reversible dehydration/hydration when heated and pulsed with water vapor at room temperature, which causes the coordination of water with zinc species [50]. The water may cause a hydration of the zinc sites, which modifies the activity of these active sites.

4. Conclusions

In this work we showed the addition of zinc and gallium changes the acidic properties of the ZSM-5 in different ways. Zinc is more effective at exchanging with the protons at the Brønsted acid sites than gallium (0.5Zn/ZSM-5 has 33% less Brønsted acid sites than 5Ga/ZSM-5). The addition of these metals creates Lewis acidity. This Lewis acidity is likely due to exchanged, dispersed extra-framework, or surfaces bulk species.

The addition of gallium or zinc to ZSM-5 catalysts promotes the conversion of furan into aromatic products. Both metals promote decarbonylation of furan, but this is more noticeable with zinc promoted ZSM-5, which shows a CO selectivity about 5% greater than the gallium promoted ZSM-5, at 5 wt% metal loading. Both of these metals also increase selectivity towards allene and benzene, but this effect is

considerably greater with Zn/ZSM-5 than Ga/ZSM-5. At 5 wt% metal loading, there is a difference of 17.5% in allene selectivity between Zn/ZSM-5 and Ga/ZSM-5; similarly, there is a difference of 25.4% for benzene selectivity. The Zn/ZSM-5 catalysts have higher activity than Ga/ZSM-5 for both furan decarbonylation (producing CO and allene), and aromatization of allene to benzene, at the same metal loadings. Considering how various products may scale with acid sites reveals that increasing the amount of Lewis acid sites increases the aromatic yield of furan conversion over Ga/ZSM-5 or Zn/ZSM-5.

The addition of zinc to ZSM-5 decreased the effects of water on furan hydrolysis (higher rates of furan hydrolysis to propylene and CO_2). An increase in the methane yield with the addition of zinc to ZSM-5 was observed when furan was co-fed with water.

Declaration of competing interest

The authors declare the following financial interests/personal relationships which may be considered as potential competing interests: George W Huber has financial interest in Anellotech which is commercializing a technology to produce aromatics from wood.

Acknowledgements

This work was supported financially by the National Science Foundation Office of Emerging Frontiers in Research and Innovation (EFRI), United States of America, grant number 0937895 and the National Council for Scientific and Technological Development (CNPq), Brazil.

Appendix A. Supplementary data

Supplementary data to this article can be found online at https://doi.org/10.1016/j.fuproc.2019.106319.

References

[1] R.H. Venderbosch, A critical view on catalytic pyrolysis of biomass, ChemSusChem. 8 (2015) 1306–1316, https://doi.org/10.1002/cssc.201500115.
[2] S. Kelkar, C.M. Saffron, K. Andreassi, Z. Li, A. Murkute, D.J. Miller, et al., A survey of catalysts for aromatics from fast pyrolysis of biomass, Appl. Catal. B Environ. 174–175 (2015) 85–95, https://doi.org/10.1016/j.apcatb.2015.02.020.
[3] S.D. Stefanidis, K.G. Kalogiannis, E.F. Iliopoulou, A.A. Lappas, P.A. Pilavachi, In-situ upgrading of biomass pyrolysis vapors: catalyst screening on a fixed bed reactor, Bioresour. Technol. 102 (2011) 8261–8267, https://doi.org/10.1016/j.biortech.2011.06.032.
[4] D. Castello, S. He, M.P. Ruiz, R.J.M. Westerhof, H.J. Heeres, K. Seshan, et al., Is it possible to increase the oil yield of catalytic pyrolysis of biomass? A study using commercially-available acid and basic catalysts in ex-situ and in-situ modus, J. Anal. Appl. Pyrolysis 137 (2019) 77–85, https://doi.org/10.1016/J.JAAP.2018.11.012.
[5] R. Thilakaratne, T. Brown, Y. Li, G. Hu, R. Brown, Mild catalytic pyrolysis of biomass for production of transportation fuels: a techno-economic analysis, Green Chem. 16 (2014) 627, https://doi.org/10.1039/c3gc41314d.
[6] G.T. Neumann, J.C. Hicks, Novel hierarchical cerium-incorporated MFI zeolite catalysts for the catalytic fast pyrolysis of lignocellulosic biomass, ACS Catal. 2 (2012) 642–646, https://doi.org/10.1021/cs200648q.
[7] A.V. Bridgwater, Review of fast pyrolysis of biomass and product upgrading, Biomass and Bioenergy 38 (2012) 68–94, https://doi.org/10.1016/j.biombioe.2011.01.048.
[8] S.P.R. Katikaneni, J.D. Adjaye, N.N. Bakhshi, Studies on the catalytic conversion of canola oil to hydrocarbons: influence of hybrid catalysts and steam, Energy Fuel 9 (1995) 599–609, https://doi.org/10.1021/ef00052a005.
[9] G.W. Huber, A. Corma, Synergies between bio- and oil refineries for the production of fuels from biomass, Angew. Chem. Int. Ed. 46 (2007) 7184–7201, https://doi.org/10.1002/anie.200604504.
[10] G.W. Huber, S. Iborra, A. Corma, Synthesis of transportation fuels from biomass: chemistry, catalysts, and engineering, Chem. Rev. 106 (2006) 4044–4098, https://doi.org/10.1021/cr068360d.
[11] T.C. Hoff, D.W. Gardner, R. Thilakaratne, K. Wang, T.W. Hansen, R.C. Brown, et al., Tailoring ZSM-5 zeolites for the fast pyrolysis of biomass to aromatic hydrocarbons, ChemSusChem. (2016) 1–11, https://doi.org/10.1002/cssc.201600186.
[12] T.R. Brown, Y. Zhang, G. Hu, R.C. Brown, Techno-economic analysis of biobased chemicals production via integrated catalytic processing, Biofuels Bioprod. Biorefin. 6 (2012) 73–87, https://doi.org/10.1002/bbb.344.
[13] Q. Che, M. Yang, X. Wang, X. Chen, W. Chen, Q. Yang, et al., Aromatics production with metal oxides and ZSM-5 as catalysts in catalytic pyrolysis of wood sawdust, Fuel Process. Technol. 188 (2019) 146–152, https://doi.org/10.1016/J.FUPROC.2019.02.016.
[14] P.A. Horne, P.T. Williams, The effect of zeolite ZSM-5 catalyst deactivation during the upgrading of biomass-derived pyrolysis vapours, J. Anal. Appl. Pyrolysis 34 (1995) 65–85, https://doi.org/10.1016/0165-2370(94)00875-2.
[15] R. Coolman, G. Huber, H. Wang, H. Chen, H. Yang, W. Fan, et al., The effects of contact time and coking on the catalytic fast pyrolysis of cellulose, Green Chem. 19 (2016) 286–297, https://doi.org/10.1039/c6gc02239a.
[16] P.A. Horne, P.T. Williams, Upgrading of biomass-derived pyrolytic vapours over zeolite ZSM-5 catalyst: effect of catalyst dilution on product yields, Fuel. 75 (1996) 1043–1050, https://doi.org/10.1016/0016-2361(96)00082-8.
[17] A.A. Lappas, M.C. Samolada, D.K. Iatridis, S.S. Voutetakis, I.A. Vasalos, Biomass pyrolysis in a circulating fluid bed reactor for the production of fuels and chemicals, Fuel. 81 (2002) 2087–2095, https://doi.org/10.1016/S0016-2361(02)00195-3.
[18] X. Zhang, H. Lei, S. Chen, J. Wu, Catalytic *co*-pyrolysis of lignocellulosic biomass with polymers: a critical review, Green Chem. 18 (2016) 4145–4169, https://doi.org/10.1039/c6gc00911e.
[19] M.M. Rahman, R. Liu, J. Cai, Catalytic fast pyrolysis of biomass over zeolites for high quality bio-oil – a review, Fuel Process. Technol. 180 (2018) 32–46, https://doi.org/10.1016/j.fuproc.2018.08.002.
[20] A. Zheng, L. Jiang, Z. Zhao, Z. Huang, K. Zhao, G. Wei, Catalytic fast pyrolysis of lignocellulosic biomass for aromatic production: chemistry, catalyst and process, WIREs Energy Environ. (2016) 1–18, https://doi.org/10.1002/wene.234.
[21] R. French, S. Czernik, Catalytic pyrolysis of biomass for biofuels production, Fuel Process. Technol. 91 (2010) 25–32, https://doi.org/10.1016/j.fuproc.2009.08.011.
[22] K. Wang, K.H. Kim, R.C. Brown, Catalytic pyrolysis of individual components of lignocellulosic biomass, Green Chem. 16 (2014) 727–735, https://doi.org/10.1039/c3gc41288a.
[23] A. Galadima, O. Muraza, In situ fast pyrolysis of biomass with zeolite catalysts for bioaromatics/gasoline production: a review, Energy Convers. Manag. 105 (2015) 338–354, https://doi.org/10.1016/j.enconman.2015.07.078.
[24] T.R. Carlson, Y.-T. Cheng, J. Jae, G.W. Huber, Production of green aromatics and olefins by catalytic fast pyrolysis of wood sawdust, Energy Environ. Sci. 4 (2011) 145–161, https://doi.org/10.1039/c0ee00341g.
[25] T.R. Carlson, J. Jae, Y.-C. Lin, G.A. Tompsett, G.W. Huber, Catalytic fast pyrolysis of glucose with HZSM-5: the combined homogeneous and heterogeneous reactions, J. Catal. 270 (2010) 110–124, https://doi.org/10.1016/j.jcat.2009.12.013.
[26] J. Cho, J.M. Davis, G.W. Huber, The intrinsic kinetics and heats of reactions for cellulose pyrolysis and char formation, ChemSusChem. 3 (2010) 1162–1165, https://doi.org/10.1002/cssc.201000119.
[27] T.R. Carlson, G.A. Tompsett, W.C. Conner, G.W. Huber, Aromatic production from catalytic fast pyrolysis of biomass-derived feedstocks, Top. Catal. 52 (2009) 241–252, https://doi.org/10.1007/s11244-008-9160-6.
[28] Y.-T. Cheng, G.W. Huber, Production of targeted aromatics by using Diels–Alder classes of reactions with furans and olefins over ZSM-5, Green Chem. 14 (2012) 3114, https://doi.org/10.1039/c2gc35767d.
[29] Y.-T. Cheng, J. Jae, J. Shi, W. Fan, G.W. Huber, Production of renewable aromatic compounds by catalytic fast pyrolysis of lignocellulosic biomass with bifunctional Ga/ZSM-5 catalysts, Angew. Chem. 124 (2012) 1416–1419, https://doi.org/10.1002/ange.201107390.
[30] Y.-T. Cheng, G.W. Huber, Chemistry of furan conversion into aromatics and olefins over HZSM-5: a model biomass conversion reaction, ACS Catal. 1 (2011) 611–628, https://doi.org/10.1021/cs200103j.
[31] E.A. Uslamin, N.A. Kosinov, E.A. Pidko, E.J.M. Hensen, Catalytic conversion of furanic compounds over Ga-modified ZSM-5 zeolites as a route to biomass-derived aromatics, Green Chem. 20 (2018) 3818–3827, https://doi.org/10.1039/c8gc01528g.
[32] J. Gou, Z. Wang, C. Li, X. Qi, V. Vattipalli, Y.T. Cheng, et al., The effects of ZSM-5 mesoporosity and morphology on the catalytic fast pyrolysis of furan, Green Chem. 19 (2017) 3549–3557, https://doi.org/10.1039/c7gc01395g.
[33] X. Qi, W. Fan, Selective production of aromatics by catalytic fast pyrolysis of furan with in situ dehydrogenation of propane, ACS Catal. 9 (2019) 2626–2632, https://doi.org/10.1021/acscatal.8b04859.
[34] J. Jae, R. Coolman, T.J. Mountziaris, G.W. Huber, Catalytic fast pyrolysis of lignocellulosic biomass in a process development unit with continual catalyst addition and removal, Chem. Eng. Sci. 108 (2014) 33–46, https://doi.org/10.1016/j.ces.2013.12.023.
[35] P.U. Karanjkar, R.J. Coolman, G.W. Huber, M.T. Blatnik, S. Almalkie, S.M. de Bruyn Kops, et al., Production of aromatics by catalytic fast pyrolysis of cellulose in a bubbling fluidized bed reactor, AICHE J. 60 (2014) 1320–1335, https://doi.org/10.1002/aic.14376.
[36] H. Zhang, T.R. Carlson, R. Xiao, G.W. Huber, Catalytic fast pyrolysis of wood and alcohol mixtures in a fluidized bed reactor, Green Chem. 14 (2012) 98, https://doi.org/10.1039/c1gc15619e.
[37] A.J. Foster, J. Jae, Y.T. Cheng, G.W. Huber, R.F. Lobo, Optimizing the aromatic yield and distribution from catalytic fast pyrolysis of biomass over ZSM-5, Appl. Catal. A Gen. 423–424 (2012) 154–161, https://doi.org/10.1016/j.apcata.2012.02.030.
[38] J. Jae, G.A. Tompsett, A.J. Foster, K.D. Hammond, S.M. Auerbach, R.F. Lobo, et al., Investigation into the shape selectivity of zeolite catalysts for biomass conversion, J. Catal. 279 (2011) 257–268, https://doi.org/10.1016/j.jcat.2011.01.019.
[39] G. Liu, M.M. Wright, Q. Zhao, R.C. Brown, Catalytic fast pyrolysis of duckweed: Effects of pyrolysis parameters and optimization of aromatic production, J. Anal. Appl. Pyrolysis 112 (2015) 29–36, https://doi.org/10.1016/j.jaap.2015.02.026.
[40] T.J.G. Kofke, R.J. Gorte, G.T. Kokotailo, Determination of framework

concentrations of gallium in [Ga]-ZSM-5, Appl. Catal. 54 (1989) 177–188, https://doi.org/10.1016/S0166-9834(00)82363-5.
[41] E.S. Shpiro, D.P. Shevchenko, M.S. Kharson, A.A. Dergachev, K.M. Minachev, Formation of strong electron—acceptor centers in reduced Ga- and Pt—Ga zeolites, Zeolites. 12 (1992) 670–673, https://doi.org/10.1016/0144-2449(92)90113-4.
[42] S.B.A. Hamid, E.G. Derouane, G. Demortier, J. Riga, M.A. Yarmo, State, activation, and migration of gallium in Ga H-MFI(Si,Al) propane aromatization catalysts, Appl. Catal. A Gen. 108 (1994) 85–96, https://doi.org/10.1016/0926-860X(94)85182-4.
[43] P. Meriaudeau, J.F. Dutel, Interaction of propane with H-ZSM-5 and Ga/H-ZSM-5 as studied by IR spectroscopy, J. Mol. Catal. A Chem. 69 (1996) 1–3 http://www.sciencedirect.com/science/article/pii/1381116995002987.
[44] P. Pal, J. Quartararo, S.B. Abd Hamid, E.G. Derouane, J.C. Védrine, P.C.M.M. Magusin, et al., A MAS NMR and DRIFT study of the Ga species in Ga/H-ZSM5 catalysts and their effect on propane ammoxidation, Can. J. Chem. 83 (2005) 574–580, https://doi.org/10.1139/v05-073.
[45] A. Ausavasukhi, T. Sooknoi, Additional Brønsted acid sites in [Ga]HZSM-5 formed by the presence of water, Appl. Catal. A Gen. 361 (2009) 93–98, https://doi.org/10.1016/j.apcata.2009.04.005.
[46] A. Ausavasukhi, T. Sooknoi, D.E. Resasco, Catalytic deoxygenation of benzaldehyde over gallium-modified ZSM-5 zeolite, J. Catal. 268 (2009) 68–78, https://doi.org/10.1016/j.jcat.2009.09.002.
[47] E.L. Schultz, C.A. Mullen, A.A. Boateng, Aromatic hydrocarbon production from eucalyptus urophylla pyrolysis over several metal-modified ZSM-5 catalysts, Energ. Technol. 5 (2017) 196–204, https://doi.org/10.1002/ente.201600206.
[48] H. Berndt, G. Lietz, J. Völter, Zinc promoted H-ZSM-5 catalysts for conversion of propane to aromatics II. Nature of the active sites and their activation, Appl. Catal. A Gen. 146 (1996) 365–379, https://doi.org/10.1016/S0926-860X(96)00124-X.
[49] H. Berndt, G. Lietz, B. Lücke, J. Völter, Zinc promoted H-ZSM-5 catalysts for conversion of propane to aromatics I. Acidity and activity, Appl. Catal. A Gen. 146 (1996) 351–363, https://doi.org/10.1016/S0926-860X(96)00092-0.
[50] J.A. Biscardi, G.D. Meitzner, E. Iglesia, Structure and density of active Zn species in Zn/H-ZSM5 propane aromatization catalysts, J. Catal. 179 (1998) 192–202, https://doi.org/10.1006/jcat.1998.2177.
[51] J.A. Biscardi, E. Iglesia, Reaction pathways and rate-determining steps in reactions of alkanes on H-ZSM5 and Zn/H-ZSM5 catalysts, J. Catal. 182 (1999) 117–128, https://doi.org/10.1006/jcat.1998.2312.
[52] V. Kanazirev, G.L. Price, K.M. Dooley, Enhancement in propane aromatization with Ga2O3/HZSM-5 catalysts, J. Chem. Soc. Chem. Commun. 3 (1990) 712, https://doi.org/10.1039/c39900000712.
[53] I. Nowak, J. Quartararo, E.G. Derouane, J.C. Vedrine, Effect of H2–O2 pre-treatments on the state of gallium in Ga/H-ZSM-5 propane aromatisation catalysts, Appl. Catal. A Gen. 251 (2003) 107–120, https://doi.org/10.1016/S0926-860X(03)00299-0.
[54] P. Meriaudeau, C. Naccache, The role of Ga2O3 and proton acidity on the dehydrogenating activity of Ga2O3-HZSM-5 catalysts: evidence of a bifunctional mechanism, J. Mol. Catal. 59 (1990) L31–L36, https://doi.org/10.1016/0304-5102(90)85100-V.
[55] P. Meriaudeau, G. Sapaly, C. Naccache, Dual function mechanism of alkane aromatization over H-ZSM-5 supported Ga, Zn, Pt catalysts: respective role of acidity and additive, Stud. Surf. Sci. Catal. 60 (1991) 267–279, https://doi.org/10.1016/S0167-2991(08)61904-7.
[56] P. Meriaudeau, S.B. Abdul Hamid, C. Naccache, Propane conversion on Ga-HZSM-5: effect of aging on the dehydrogenating and acid functions using pyridine as an IR probe, J. Catal. 139 (1993) 679–682, https://doi.org/10.1006/jcat.1993.1059.
[57] P. Mériaudeau, G. Sapaly, C. Naccache, Framework and non-framework gallium in pentasil-like zeolite as studied in the reaction of propane, J. Mol. Catal. 81 (1993) 293–300, https://doi.org/10.1016/0304-5102(93)80013-K.
[58] P. Meriaudeau, C. Naccache, Further evidence on the change of acid properties of H-ZSM-5 by Ga and Pt, J. Catal. 157 (1995) 283–288.
[59] G.J. Buckles, G.J. Hutchings, Aromatisation of propane over Ga/H-ZSM-5: comments on the activation of propane, Catal. Today 31 (1996) 233–246, https://doi.org/10.1016/S0920-5861(96)00027-2.
[60] S.B. Abdul Hamid, E.G. Derouane, P. Mériaudeau, C. Naccache, Effect of reductive and oxidative atmospheres on the propane aromatisation activity and selectivity of Ga/H-ZSM-5 catalysts, Catal. Today 31 (1996) 327–334, https://doi.org/10.1016/S0920-5861(96)00015-6.
[61] J.A. Biscardi, E. Iglesia, Structure and function of metal cations in light alkane reactions catalyzed by modified H-ZSM5, Catal. Today 31 (1996) 207–231, https://doi.org/10.1016/S0920-5861(96)00028-4.
[62] P. Meriaudeau, C. Naccache, Dehydrogenation and dehydrocyclization catalytic properties of gallium oxide, J. Mol. Catal. 50 (1989) L7–L10, https://doi.org/10.1016/0304-5102(89)80103-8.
[63] E.A. Uslamin, B. Luna-Murillo, N. Kosinov, P.C.A. Bruijnincx, E.A. Pidko, B.M. Weckhuysen, et al., Gallium-promoted HZSM-5 zeolites as efficient catalysts for the aromatization of biomass-derived furans, Chem. Eng. Sci. 198 (2019) 305–316, https://doi.org/10.1016/j.ces.2018.09.023.
[64] C.A. Mullen, P.C. Tarves, L.M. Raymundo, E.L. Schultz, A.A. Boateng, J.O. Trierweiler, Fluidized bed catalytic pyrolysis of eucalyptus over HZSM-5: effect of acid density and gallium modification on catalyst deactivation, Energy Fuel 32 (2018) 1771–1778, https://doi.org/10.1021/acs.energyfuels.7b02786.
[65] A.R. Stanton, K. Iisa, M.M. Yung, K.A. Magrini, Catalytic fast pyrolysis with metal-modified ZSM-5 catalysts in inert and hydrogen atmospheres, J. Anal. Appl. Pyrolysis 135 (2018) 199–208, https://doi.org/10.1016/j.jaap.2018.09.002.
[66] Y. Zheng, F. Wang, X. Yang, Y. Huang, C. Liu, Z. Zheng, et al., Study on aromatics production via the catalytic pyrolysis vapor upgrading of biomass using metal-loaded modified H-ZSM-5, J. Anal. Appl. Pyrolysis 126 (2017) 169–179, https://doi.org/10.1016/j.jaap.2017.06.011.
[67] W.-L. Fanchiang, Y.-C. Lin, Catalytic fast pyrolysis of furfural over H-ZSM-5 and Zn/H-ZSM-5 catalysts, Appl. Catal. A Gen. 419–420 (2012) 102–110, https://doi.org/10.1016/j.apcata.2012.01.017.
[68] J.M. Coronado, J. Čejka, P. Jana, P. Pizarro, J. Fermoso, H. Hernando, et al., Lamellar and pillared ZSM-5 zeolites modified with MgO and ZnO for catalytic fast-pyrolysis of eucalyptus woodchips, Catal. Today 277 (2016) 171–181, https://doi.org/10.1016/j.cattod.2015.12.009.
[69] R. Chang, L. Zhu, F. Jin, M. Fan, J. Liu, Q. Jia, et al., Production of bio-based p-xylene via catalytic pyrolysis of biomass over metal oxide-modified HZSM-5 zeolites, J. Chem. Technol. Biotechnol. 93 (2018) 3292–3301, https://doi.org/10.1002/jctb.5691.
[70] F.M. Mayer, C.M. Teixeira, J.G.A. Pacheco, C.T. de Souza, D. de V. Bauer, E.B. Caramão, et al., Characterization of analytical fast pyrolysis vapors of medium-density fiberboard (mdf) using metal-modified HZSM-5, J. Anal. Appl. Pyrolysis. 136 (2018) 87–95, https://doi.org/10.1016/j.jaap.2018.10.019.
[71] Q. Che, M. Yang, L. Rose Williams, Y. Zhu, Q. Yang, J. Zou, et al., Influence of physicochemical properties of metal modified ZSM-5 catalyst on benzene, toluene and xylene production from biomass catalytic pyrolysis, Bioresour. Technol. 278 (2019) 248–254, https://doi.org/10.1016/j.biortech.2019.01.081.
[72] C.J. Gilbert, J.S. Espindola, W.C. Conner, J.O. Trierweiler, G.W. Huber, The effect of water on furan conversion over ZSM-5, ChemCatChem. 6 (2014) 2497–2500, https://doi.org/10.1002/cctc.201402390.
[73] E.J.M. Hensen, E.A. Pidko, N. Rane, R.A. van Santen, Water-promoted hydrocarbon activation catalyzed by binuclear gallium sites in ZSM-5 zeolite, Angew. Chem. Int. Ed. Engl. 46 (2007) 7273–7276, https://doi.org/10.1002/anie.200702463.
[74] T.J. Kofke, R.J. Gorte, G.T. Kokotailo, W.E. Farneth, Stoichiometric adsorption complexes in H-ZSM-5, H-ZSM-12, and H-mordenite zeolites, J. Catal. 115 (1989) 265–272, https://doi.org/10.1016/0021-9517(89)90027-4.